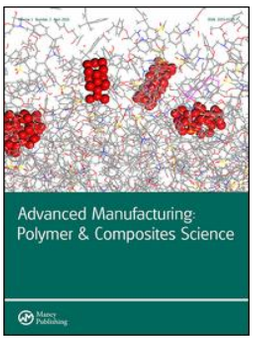


!"" !#$! % & !"" !#"' %( * & ) * ++,,,- - + + !

.

/ /

0 1 2 3 4 5*

5 * !"# $
% % & ' ' ( )
( * % + , ) - ( !+! !. " /0+
! 1!!234 "" 5"3!671 5

5 6 *



' ## , & 1 ( ( 3 %)) %( ( )%( " 3
+++ %( 3 (# ( ) , %) ( / (%#4(3 ,% (5/ (%#1 6$% ,

AMPCS Advanced Manufacturing: Polymer & Composites Science

Original Research Paper

# Electric field induced alignment of multiwalled carbon nanotubes in polymers and multiscale composites

Maxime Arguin[1], Frédéric Sirois*[2] and Daniel Therriault[1]

[1]Laboratory for Multiscale Mechanics, Mechanical Engineering Department, Polytechnique Montréal, C.P. 6079, succ. Centre-Ville, Montréal, QC H3C 3A7, Canada

[2]Laboratory in Electrical energy, Electrical Engineering Department, Polytechnique Montréal, C.P. 6079, succ. Centre-Ville, Montréal, QC H3C 3A7, Canada

Abstract Carbon fiber reinforced polymers (CFRPs) have a highly anisotropic electrical resistivity, which limits their use in electrical applications. In this contribution, an electric field was used to align multiwalled carbon nanotubes (MWCNTs) to create preferential conductive pathways within a nanocomposite and a multiscale composite in order to reduce their resistivity. Investigation on epoxy containing MWCNTs have shown that an electric field of 40 V mm$^{2\,1}$ or higher applied for 2 h can lead to a reduction of the resistivity parallel to the field up to four orders of magnitude with only 0.01 wt-% loading. In the case of CFRPs reinforced with 0.01 and 0.1 wt-% of MWCNTs, we observed reductions of the through the thickness resistivity of 36 and 99% respectively, when an electric field of 60 V mm$^{2\,1}$ was applied for 2 h during the fabrication of the samples.

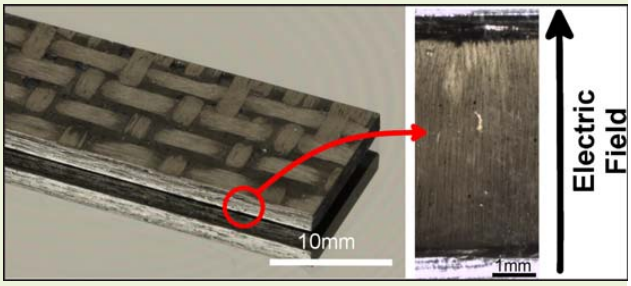


Keywords Carbon nanotubes, Nanocomposites, Multiscale composites, Electrical properties, Alignment

Cite this article M. Arguin, F. Sirois and D. Therriault: Adv. Manuf.: Polym. Compos. Sci., 2015, 1, 16-25

## Introduction

With increasing cost of fuel, energy ef“ciency has become a major requirement for new aircraft designs, which has led to signi“cant efforts for reducing their weight. On the one hand, composite structures progressively replace aluminum ones, and on the other hand, more and more electrical devices are being installed in replacement of their heavier mechanical counterpart. A well known bottleneck of the combination of these approaches is that the aluminum fuselage, which was traditionally used as the current return network for the electrical devices, is now replaced with carbon “ber reinforced polymers (CFRPs). However, the electrical resistivity of these materials is more than six orders of magnitude higher, and therefore CFRPs cannot be used as a reliable current return path in day of today[1].

The real problem is that, even though carbon “bers are reasonably conductive and could in principle be used to some extent in the current return network, their integration into a polymer resin for forming CFRP panels greatly increases the overall bulk resistivity of the composite assembly. The resin also creates undesirable anisotropy of electrical properties since the resistivity measured through the thickness of CFRP panels was shown to be 1000 times higher than that measured in the plane of the “bers[2]. As a consequence, when an electric current is injected in a CFRP panel, it cannot diffuse through the thickness and stays in the surface plies, generating heat and thus leading to a faster degradation of the material.

Carbon nanotubes (CNTs) have demonstrated their potential for the enhancement of mechanical and electrical properties of CFRPs to create multiscale composites, which is de“ned as the combination of micro-reinforcements (carbon “bers) and nanoreinforcements (CNTs). A review paper from Chou et al. demonstrated different approaches to use CNTs from one-dimensional “ber to three-dimensional dispersion into a polymer matrix[3]. In polymer materials, it has been demonstrated that CNTs can signi“cantly improve the electrical properties even at a very low concentrations[4–6]. In that case, the resistivity of the nanocomposites is mainly

*Corresponding author, email f.sirois@polymtl.ca



Received 14 July 2014; accepted 17 November 2014
DOI 10.1179/2055035914Y.0000000003



Maney Publishing

related to the formation of a percolation network within the material. The high aspect ratio of the CNTs and their appropriate dispersion into the resin are the main factors to reach a low percolation threshold.[6–8]

Two main approaches are possible for incorporating CNTs into a CFRP: (i) CNT deposition on the "bers and (ii) CNT dispersion into the matrix.[9] Different techniques to attach CNTs on "ber such as chemical vapor deposition (CVD),[10] electrophoresis deposition[11] or agglomeration of CNTs by sizing agents[12] have shown signi"cant improvements in the electrical and mechanical properties. For example, Yamamoto et al.[13] have reduced the resistivity of alumina "ber composite by six orders of magnitude, reaching a through the thickness (TT) resistivity of 0.07 Ω m (13 S m$^{-1}$) with 3 wt-% of CNTs using the CVD technique to modify the "bers. Glass "ber multiscale composites modi"ed with a sizing agent studied by Gao et al.[14] have reached a resistivity of y 10 Ω m (10$^{2.1}$ S m$^{-1}$), which is four orders of magnitude lower than multiscale composites made by three-roll milling (y 10$^{2.5}$ S m$^{-1}$). However, the CVD and electrophoresis deposition processes could hardly be adapted to fast production rates required in the industry and may also lead to a degradation of the "bers.[9] The use of a CNT modi"ed matrix has the advantage of being more compatible with traditional industrial processes, in addition to increase the interlaminar shear strength as well as the electrical conductivity of the composite material.[14–17] However, this approach shows moderate performance because it is limited to low CNT loadings. At high CNT loading (. 1 wt-%), the viscosity of the resin considerably increases, which leads to an inhomogeneous dispersion of the particles due to "ltration and incomplete impregnation of the "bers.[18]

It is important to control well the dispersion of the particles into the polymer in order to maximize the improvement in electrical performances for a given CNT loading. This is achieved by creating electrically conductive pathways, which can be either percolation paths (when very low concentrations of CNTs are used), or direct conduction paths, requiring that the CNTs touch each other all along the path, which is possible only at higher concentrations of particles.

It is known from the literature that an electric "eld enables the movement of the CNTs to form percolation networks. For example, Khan et al.[19] have used an electric "eld to lower the percolation threshold to 0.0048 wt-%, which is one order of magnitude less than the case of randomly dispersed CNTs. According to Oliva-Avilese et al. and Monti et al.,[20,21] the reduction of the resistivity is the result of dielectrophoretic forces that contribute to align the particle in the direction of the electric "eld. Other studies improve the electrical properties of polymers in a preferential direction with CNT loadings as low as 0.01 wt-%.[22–25] Park et al.[22] have reduced the resistivity of a polymer containing 0.03 wt-% of CNTs by six order of magnitude by applying an electric "eld of 200 $V_{pp}$ at a frequency of 1 kHz. The optimal parameters for the alignment were empirically found and the alignment mechanisms are still not completely understood. The use of CNTs aligned with an electric "eld to reduce the electrical resistivity of glass "ber composites has been reported,[26,27] but to the best of our knowledge, no study were performed on carbon "ber composites.

In this contribution, the objective is to reduce the electrical resistivity through the thickness of CFRPs in order to improve current diffusion through composite panels, and eventually make them reliable as current carrying parts in an aircraft or other applications. In order to achieve this goal, multiwalled carbon nanotubes (MWCNTs) dispersed into an epoxy matrix were aligned with an electric "eld during the curing stage. In the "rst part of the paper, we investigate the in"uence of the electric "eld intensity on the time required for obtaining full alignment of the particles in epoxy nanocomposites. This was a necessary step in order to tailor the process parameters. Next, we introduce a modi"ed hand layup technique that allows applying an electric "eld during the manufacturing of the composite. Then, we describe in detail the fabrication process of multiscale composite samples for two different MWCNT loadings and processed with and without electric "eld (four cases overall). Finally, we present the results of electrical properties of each case, in terms of their (1) longitudinal resistivity (i.e. parallel to the orientation of the carbon "bers) and (2) TT resistivity (i.e. perpendicular to the orientation of the carbon "bers).

## Numerical simulations of current injection in composite panels

The high anisotropy of the electrical resistivity of CFRPs prevents their use in the current return network in aircrafts due to poor current diffusion across their thickness, which leads to undesirable heat generation. Figure 1 shows the comparison between a realistic anisotropic CFRP and an ideal isotropic material based on a 2D "nite element simulation performed using Comsol 4.3 Multiphysics. In this simulation, two different cases were analyzed. First, an anisotropic material with a resistivity ratio r$_{transverse}$/r$_{longitudinal}$ of 1000 was simulated, representing a traditional CFRP. In the second simulation, the TT resistivity (or r$_{transverse}$) was reduced to match r$_{longitudinal}$ to obtain an isotropic material (resistivity ratio of 1). In both cases, a current density of 6.4 A cm$^{-2}$ (i.e. 10 A injected on a surface of 12.5 × 12.5 mm) was injected in the composite panel using a copper electrode place at the top left extremity of the material, while the other end was set to 0 V (ground potential). The simulation outputs are the current density (A cm$^{-2}$), schematically shown by the red arrows, and the power density (W mm$^{-3}$), corresponding to the Joule losses, and represented by the gray scale shaded plot.

The simulation results for the anisotropic material showed that the current (arrows) hardly diffuse through the thickness, but rather stay at the surface. This leads to heat generation by Joule effect, corresponding to the highly dissipative zone located below the electrode. When the resistivity is taken as isotropic (i.e. r$_{transverse}$ = r$_{longitudinal}$), the current is able to diffuse through the whole thickness of the material, as shown by the uniform arrows in Fig. 1b. The effective area for conduction is then signi"cantly larger as compared with the anisotropic case, and the high power dissipation mentioned above is not present anymore.

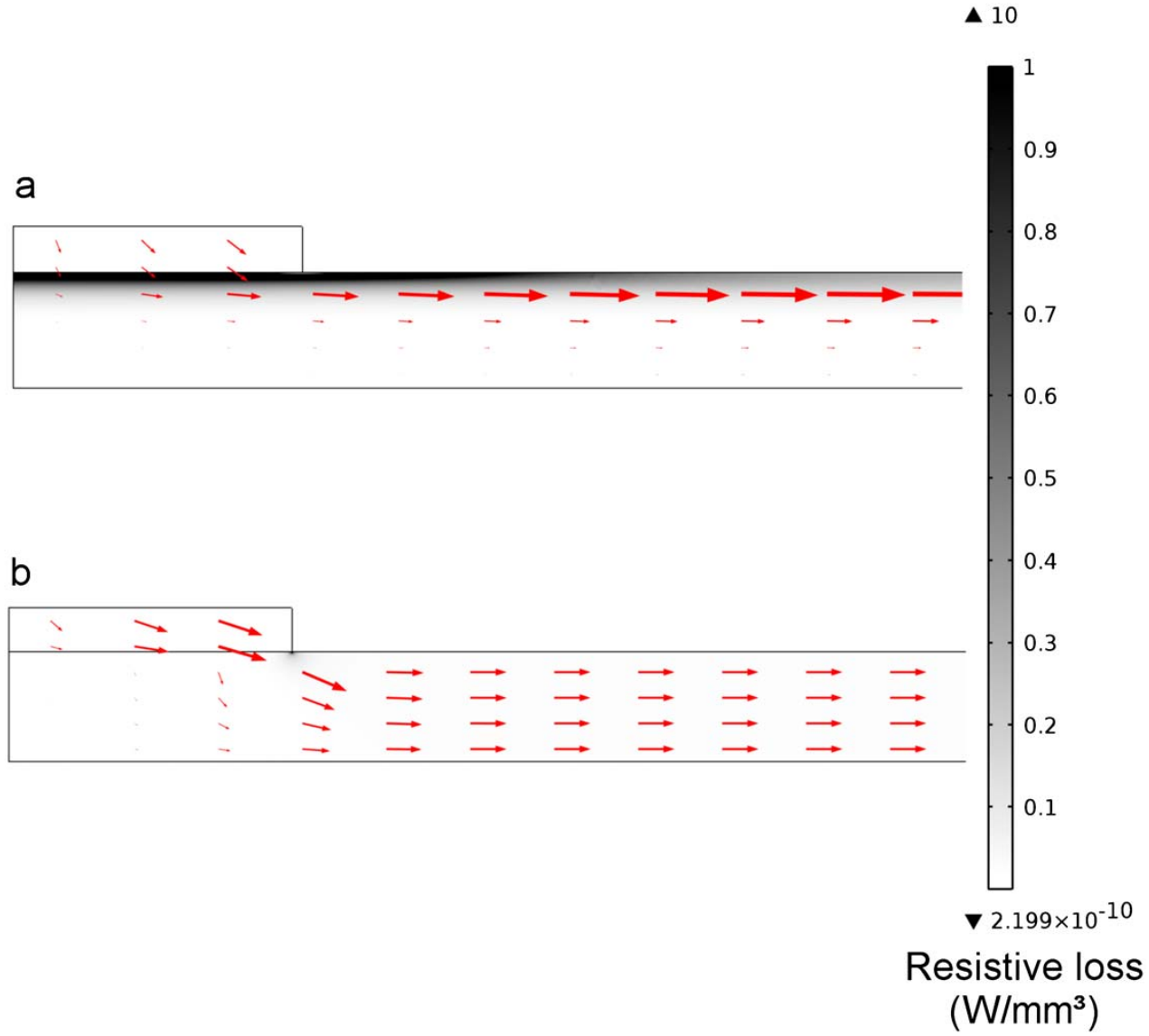


Figure 1 Numerical simulation of current density (arro ws) and resistive heat generation (gray tones) for a realistic anisotropic composite ( $r_{transverse}/r_{longitudinal}$ 5 1000) and b ideal isotropic material

# Experimental methods

## Alignment in polymer

### Nanocomposite preparation

MWCNTs (NC7000; Nanocyl) have been incorporated into a one-part UV curable epoxy (OG115; Epoxy Technology) to create nanocomposites at 0.01 and 0.1 wt-% concentrations. This epoxy has a low viscosity and is able to cure with 365 nm wavelength UV light. The MWCNTs and epoxy mixture was placed in a sonication bath (Model 8891; Cole-Parmer) for 1 h to disperse the nanotubes. The mixture was then degassed under a vacuum (Model MZ 2C NT; Vacuubrand) fory 30 min, until all bubbles entrapped in the mixture disappeared. Finally, the mixture was poured into a UV protected syringe (3cc barrel; EFD) in order to protect the epoxy from ambient light.

### Alignment of nanotubes

The nanocomposite mixture was deposited into a mold composed of two aluminium electrodes “xed to a glass substrate, as shown in Fig.a2 The purpose of this mold was to perform preliminary experiments of electric “eld alignment of the nanoparticules in order to determine the best set of experimental parameters. A constant distance of 5 mm between the electrodes was ensured with glass walls cut from a microscope slide with a precision saw (Isomet low speed precision saw; Buehler). Finally, a glass substrate was put on the top of the mold to make sure we have a ”at top surface at all times, which facilitates optical monitoring during the whole process. To generate an AC electric “eld, the mold was connected to a waveform generator (Model 2720; TEGAM), whose output voltage was ampli“ed one hundred times by the combination of a power ampli“er (Model 7796; AE Techron) and a step-up transformer (Model MO200J; Marcus).

Before applying the electric “eld, a release agent was sprayed on the mold. Then, the nanocomposite mixture was poured into the mold using the 3 cc syringe and a microscope slide was placed on the top of the mold while making sure that no air was trapped inside the mold. Afterwards, seven different electric “eld intensities were generated, namely, 20, 30, 40, 50, 60, 80 and 100 V mm$^{-1}$

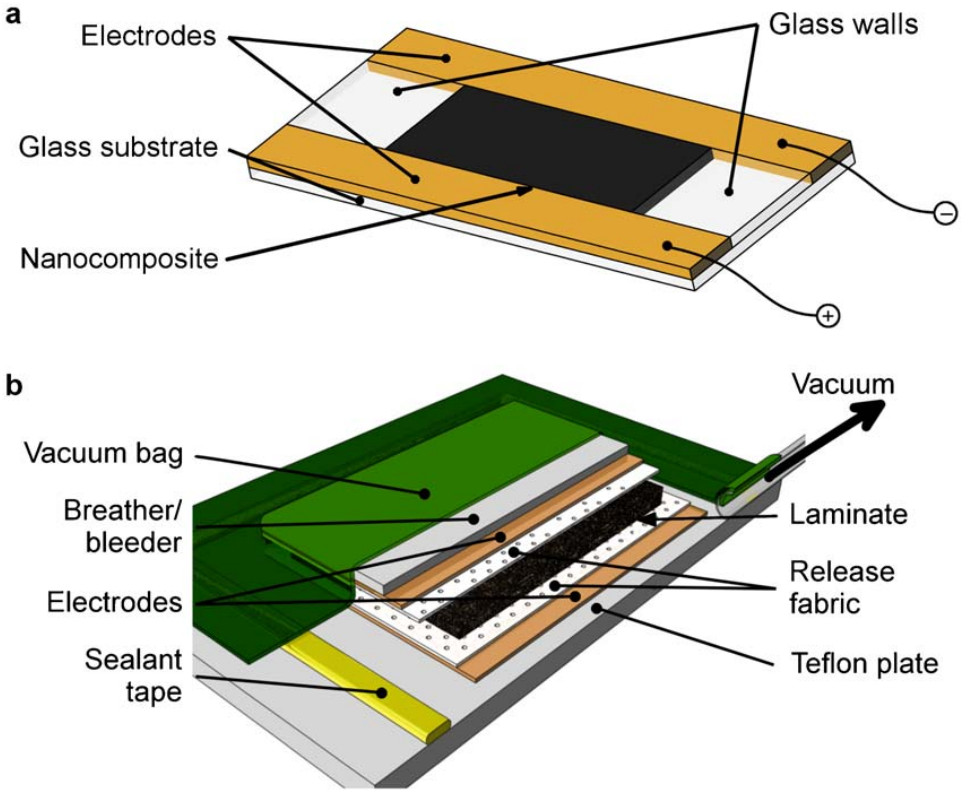


Figure 2 Schematic of a mold used for electric "eld alignment in nanocomposite and b stacking sequence of modi"ed hand layup process used for ma nufacturing of multiscale co mposites in which the nanoparticles were aligned with electric "eld during manufacturing

(corresponding to output voltages of 100, 150, 200, 250, 300, 400 and 500 V respectively). A frequency of 1 kHz has been selected for all samples, based on the observations of Park et al.[22] about the impact of the electric "eld frequency on the quality of the alignment. During the experiments, the current was measured in real time during the whole alignment process using a custom measurement set-up based on a data acquisition card (PCI-6052E; National Instrument) controlled by Labview (Labview 2009; National Instrument). The waveform generator was turned on to generate the AC electric "eld. After 2 h, the nanocomposite was cured using a UV lamp (Model B 100AP; Blak-Ray) while keeping the electric "eld on. The waveform generator was shut down only when the epoxy was totally cured, i.e. after half an hour of UV exposure.

## Electrical characterization

Figure 3a shows a picture of the sample holder designed for the electrical characterization of the nanocomposite samples. The holder is made of two electrodes between which the sample is placed. Four plastic screws are used to apply uniform pressure on the sample. A high resistance electrometer (Model 6517B; Keithley) was used to measure the electrical resistivity of the sample.

Before the measurements, each sample was "rst cut to a dimension of 56 206 1 mm with the precision saw. A "at surface "nished was obtained with a polisher (Metaserv 2000; Buehler). To reduce the contact resistance between the sample and the electrodes, a silver ink was prepared, inspired from an earlier study of Walker and Lewis.[28] The samples were placed between the electrodes and the screws were tightened by hand. A square wave voltage signal of 100 V peak and frequency of 0.1 Hz was applied for 60 s while measuring the current "owing through the sample. These measurements were repeated six times on each sample in both directions, parallel and perpendicular to the electric "eld, by manually rotating the sample inside the holder.


Figure 3 a sample holder used for electrical characterization of (i) nanocomposite samples in directions parallel and perpendicular to electric "eld and (ii) multiscale composite samples in direction par allel to electric "eld, i.e. through thickness (TT) of sample; b sample holder used for electrical characterization of multiscale composite samples in longitudinal direction, i.e. along length of samples (parallel to carbon "bers)

### Optical characterization

We performed in situ optical characterization of the electric "eld alignment of the MWCNTs in our nanocomposite samples with the help of a stereomicroscope (SZ61; Olympus). The electric "eld was applied at all times during the optical observations. A camera (In"nity 1; Lumenera) was used to take pictures every 30 s in order to monitor the displacement of the MWCNTs. Optical microscopy was also performed on fully cured sample using a microscope (SZX12; Olympus) connected to a camera (Evolution VF; Media Cybernatics).

## Multiscale composite fabrication

### Preparation of nanocomposite matrix

For the fabrication of the multiscale composite samples, the MWCNTs (NC7000; Nanocyl) were "rst mixed with acetone and the mixture was placed for 30 min in a sonication bath (Model 8891; Cole-Parmer). Next, a low viscosity aerospace-grade epoxy resin (EPON862, Miller Stephenson) without the hardener was added to the solvent mixture. The nanocomposite resin was then stirred at 50°C with a magnetic mixer (Model SP131825; Barnstead International) for 48 h to make sure that the solvent had completely evaporated. After that, the mixture was passed twice in a three-roll mixer (Model 80E/158; EXAKT) at a speed of 250 rev min$^{-1}$ and a distance between the roll of 15 mm in order to decrease aggregate size. Then, 45 phr of hardener (Epikure 3274; Momentive), chosen for its gel time of approximately 5 h at room temperature with the Epon 862 resin, were added to the epoxy. Finally, the resin was degassed under vacuum for 45 min.

### Composite manufacturing process

We have modi"ed the classical hand layup process by incorporating metal electrodes into the mold in order to apply an electric "eld during the fabrication of the multiscale composite samples. Figure 2 shows a schematic of the stacking of the different constituents in the hand layup process. First, a te"on plate was used as a base. Then, the lower electrode was stacked, followed by a porous release fabric (Model 879; West System). The release fabric is very important in the manufacturing process as it prevents the panel to stick on the electrodes after curing. It also prevents direct electrical contact of the electrodes with the laminate while keeping an electrical contact with the MWCNT reinforced matrix. Afterward, three plies of a balanced plain weave carbon fabric (Injectex GF420-E01-100; Hexcel) were stacked, and a layer of nanocomposite matrix was applied with a paint brush between each ply. Then, another release fabric was placed on the impregnated "bers followed by the upper electrode. Finally, a breather/bleeder fabric was stacked on the top to absorb the extra resin, followed by the vacuum port on (one side of the mold) and a vacuum bagging.

A vacuum was established inside the bag with a vacuum pump (Model MZ 2C NT; Vacuubrand) to compact the "bers. After complete impregnation of the laminate (~ 2 h), an AC voltage of 105 V was applied to generate an electric "eld of 60 V mm$^{-1}$ between the electrodes. The signal was generated in exactly the same way as for the alignment characterization inside the UV curable polymer (voltage of 105 V and frequency of 1 kHz). The electric "eld was applied for 2 h. Four different cases were tested: two concentrations of MWCNTs inside the matrix (i.e. 0.01 and 0.1 wt-%), with and without an electric "eld of 60 V mm$^{-1}$. Three panels were made for each condition, for a total of 12 samples. Finally, the volume "ber fraction of each sample panel was measured based on ASTM D3171.

### DC electrical characterization

Before carrying on the electrical measurements, each sample panel was cut in two samples of 66 × 12.5 mm with a precision saw (Isomet low speed saw; Buehler). The thickness of the panels was ~ 1.3 mm. The surfaces of the samples were then polished (Metaserv 2000; Buehler) with a 420 grit sand paper in order to expose the carbon "bers.

Figure 3 shows the sample holders used for the electrical characterization of the samples in both the TT and longitudinal directions. In the case of longitudinal measurements, the sample is positioned under two electrodes (one at each extremity). Four probes where used to measure the voltage at different locations along the sample. With this technique, the contact resistance between the electrodes and the sample does not in"uence the measurements. In the TT direction, the conductivity was measured using the same technique than for nanocomposite characterization explained before. For both directions, different currents from 0 to 2 A by steps of 0.25 A were injected in the sample using a DC power supply (Model GPS-3303; GW Instek) and the voltages between each pair of probes were measured with an acquisition card (PCI-6052E; National Instrument) and the Labview software (Labview 2009; National Instrument). Finally, the electrical resistance was calculated using a linear regression of the measured $I$–$V$ curve (data not shown here).

# Results and discussion

## Alignment in polymer

In view of selecting the right experimental electric "eld parameters (intensity, frequency, duration) for aligning the MWCNT particles in our multiscale composite samples, we performed a series of initial alignment tests on nanocomposite samples made of UV epoxy and MWCNTs, as described above. The major results of the electrical characterizations performed on those nanocomposite samples are summarized in this section.

Figure 4a shows in situ measurements of the resistivity for one of the sample with a MWCNT loading of 0.01 wt-%, while an electric "eld of 80 V mm$^{-1}$ was applied. At the beginning of the experiment, the resistivity of the sample decreased until it reached a minimum of 3700 Ω m after 90 min. This decrease was followed by a moderate and gradual increase in resistivity until the UV light was turned on for curing of the polymer (end of experiment). Figure 4b–e shows optical microscopic images of the dispersion of the MWCNTs within the sample at 0, 30, 60 and 180 min respectively. A complete video is available in Supplementary Material 1 http://dx.doi.org/10.1179/2055035914Y.0000000003.s1. We observed that for the "rst 60 min, there was formation of vertical "lamentary structures from one electrode to the other due to the motion of the MWCNTs caused by the electric "eld. After 90 min, we noticed a migration of some MWCNTs toward the top electrode, followed by an overall resistivity increase. This migration decreased the MWCNT concentration near the top electrode (i.e., less conductive paths), shown by the lighter

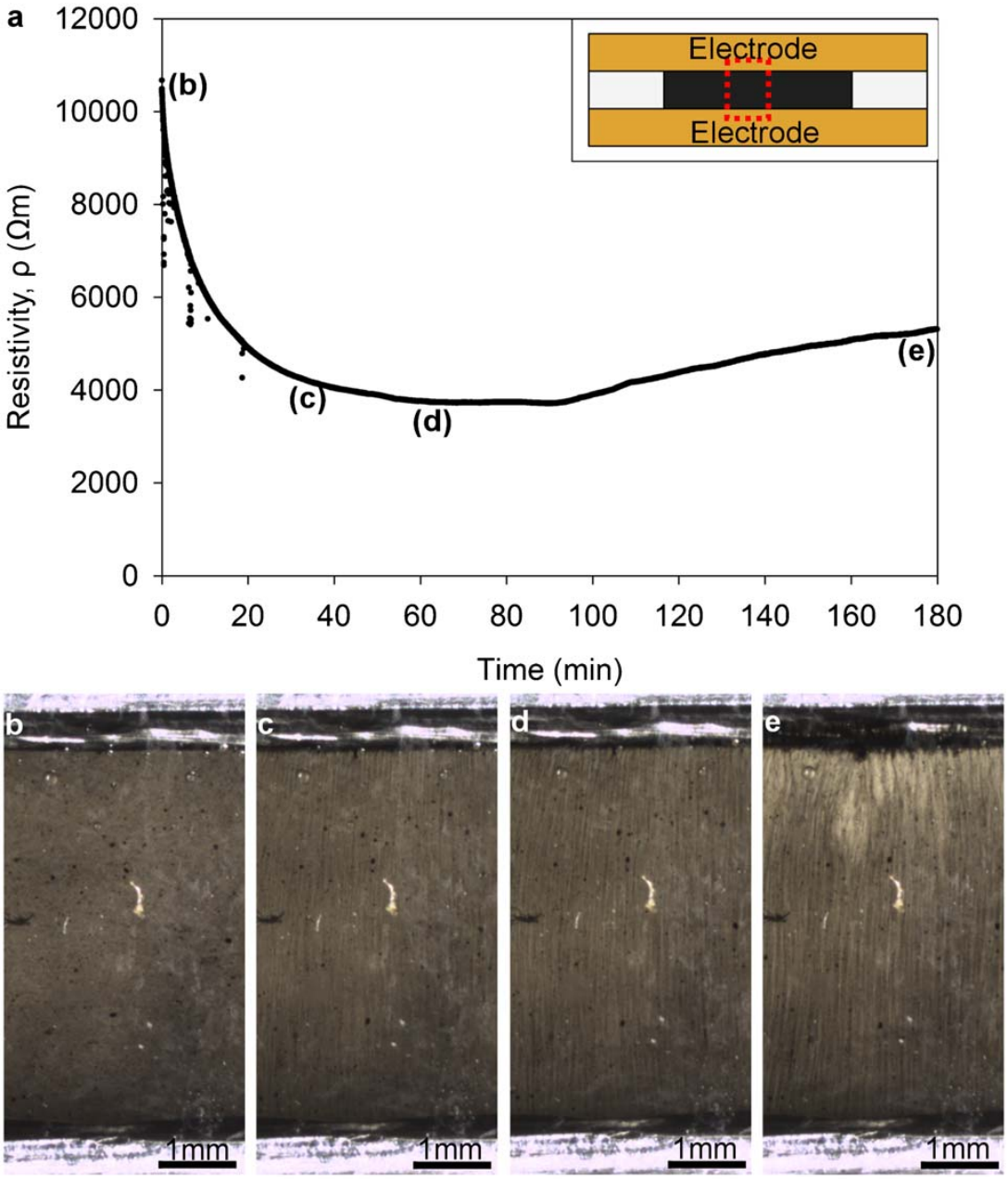


Figure 4 a In situ measurement of resistivity evolution with respect to time, while electric "eld of 80 V mm$^{-1}$ is applied on nanocomposite containing 0.01 wt-% of MWCNTs. Optical images show dispersion of MWCNTs after b 0 min, c 30 min; d 60 min and e 180 min (broken line shows zone where pictures were taken)

region in the microstructure in Fig. 4e. Experiments using different electric "eld intensities showed a similar behavior.

It is worth mentioning that the rapidity at which the "laments formed in the matrix was clearly proportional to the intensity of the electric "eld. For instance, with an electric "eld of 100 V mm$^{-1}$, the alignment process occurred faster than in the case showed in Fig. 4a and the migration also appeared faster. Conversely, for intensities of 60 V mm$^{-1}$ and below, the migration of the MWCNTs was not observed after 2 h of application of the electric "eld, and therefore, no increase of the resistivity was observed during the in-situ measurements. However, it is expected that the migration phenomenon might have occurred if the electric "eld were applied for a longer time.

In all experiments, the nanocomposite samples were fully cured with UVs before carrying on with the electrical resistivity characterization. Figure 5a shows the electrical resistivity of the UV cured nanocomposite samples with 0.01 and 0.1 wt-% MWCNT loadings processed at seven different electric "eld intensities (i.e. 20, 30, 40, 50, 60, 80 and 100 V mm$^{-1}$). Measurements performed on a benchmark sample processed without electric "eld is also shown. The resistivity values measured along the directions parallel to the electric "eld (solid symbols) and perpendicular to the electric "eld (open symbols) are shown. For samples with 0.01 wt-% MWCNT loading, the effect of the electric "eld was clearly visible in the direction parallel to the electric "eld. For an intensity of 20V mm$^{-1}$, there was no signi"cant change in the resistivity ($\rho \approx 7.8 \times 10^{7}$ Vm) when compared with the benchmark sample. This is supported by Fig. 5b and c, which show no signi"cant alignment of the MWCNT microstructure in the sample. From 30 V mm$^{-1}$, the

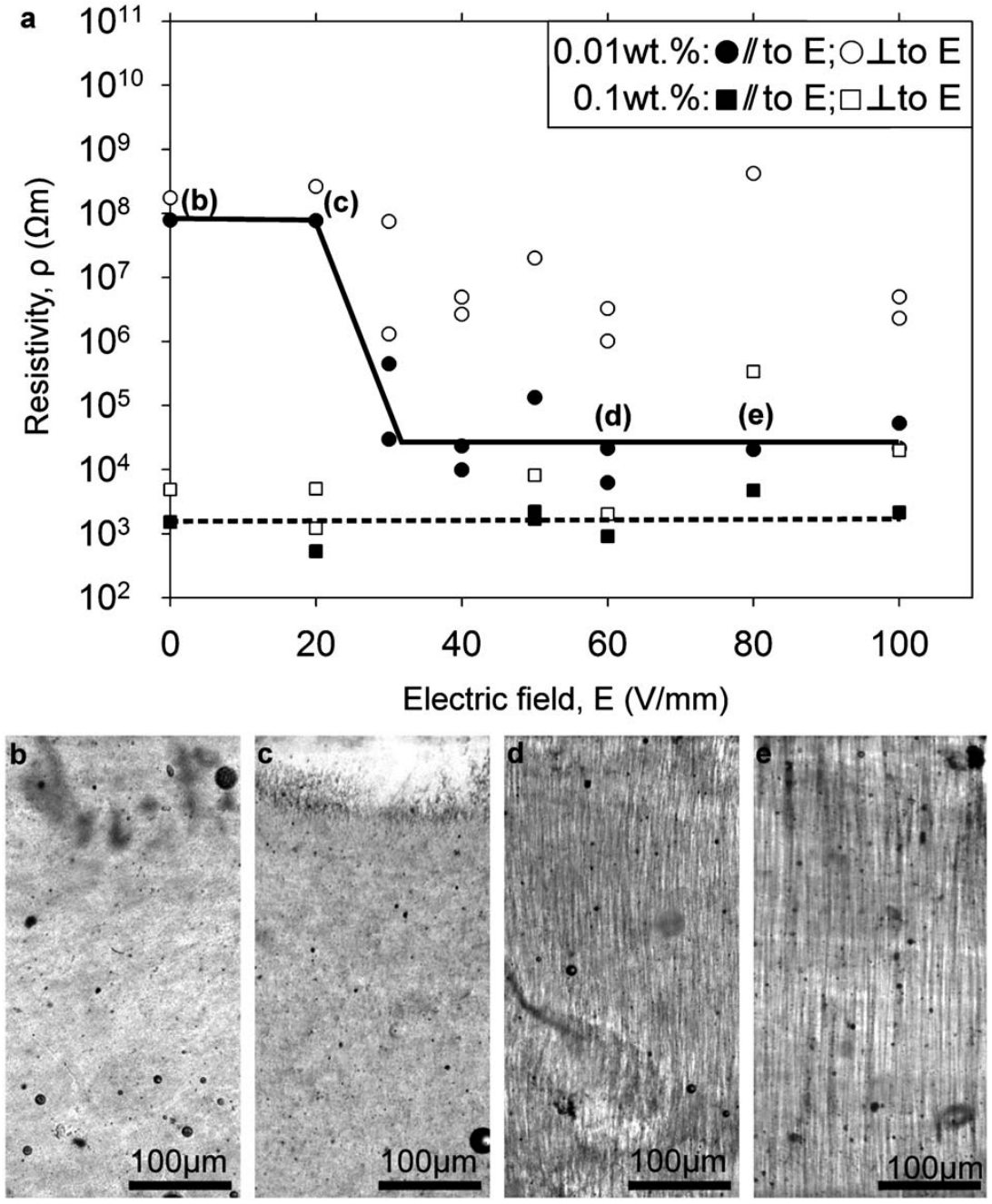


Figure 5 a Resistivity of cured nanocomposite as function of elec tric "eld intensity after 2 h application, for MWCNT loadings of 0.01 and 0.1 wt-%. Optical images show dispersion of MWCNTs with electric "elds of b 0 V mm$^{-1}$, c 20 V mm$^{-1}$, d 60 V mm$^{-1}$ and e 80 V mm$^{-1}$ applied for 2 h

resistivity parallel to electric "eld sharply decreases from y $10^{8}$ to y $10^{4}$ Vm, and saturates to a plateau for higher electric "eld intensities (the solid line shows the general trend observed for the resistivity parallel to the electric "eld orientation). Figure 5d and e shows samples realized with an electric "eld intensity of 60 and 80 V mm$^{-1}$ respectively, for which the alignment of the MWCNT particles was apparent. In the direction perpendicular to the electric "eld, there was a high dispersion of the resistivity and no general trend was observed. The variation in the measured values is mainly related to the initial dispersion of the MWCNTs into the epoxy. The randomly dispersed aggregates that join a given "lament act as bridges to connect the "laments together. Depending on the initial content of aggregates in the matrix, the nanocomposite is more or less likely to present percolation pathways perpendicular to the electric "eld. Since this is hardly controllable, resistivity dissimilarities varying from one to "ve orders of magnitude were observed in the direction perpendicular to the electric "eld (versus values measured parallel to the "eld) on samples processed with electric "elds higher than 40 V mm$^{-1}$.

For samples with MWCNT loadings of 0.1 wt-%, the impact of the electric "eld during the processing was not as signi"cant as for the 0.01 wt-% loading. In both directions (i.e. parallel and perpendicular to the electric "eld), there was no difference in the electrical resistivity for all intensities tested and for the benchmark sample (see dashed line in Fig. 5a). However, the resistivity was close to $10^{3}$ Vm, which

is low for epoxies. At 0.1 wt-%, percolation or even conduction pathways naturally forms in the nanocomposite, which explains the low resistivity measured even without applying an electric “eld. Therefore, the samples act like a resistor, with no preferential path for the current since the nanoparticles are randomly connected in all directions. The electric “eld had no apparent effect and no reduction of the resistivity was observed compared to the benchmark sample.

Based on our observations on the UV epoxy and MWCNT nanocomposites, an electric “eld intensity of 60 V mm$^{-1}$ was selected for the alignment process during the fabrication of the multiscale composite samples. This intensity was the highest intensity at which no migration of the MWCNTs toward the electrodes occurred during the alignment period (2 h), while allowing relatively quick alignment. Microscopic observations of the microstructure also clearly showed the formation of “lamentary structures that spans through the sample in the direction parallel to the electric “eld, as desired.

## Alignment in multiscale composites

Multiscale composites with a matrix containing 0.01 and 0.1 wt-% of MWCNTs were fabricated with a 60 V mm$^{-1}$ electric “eld intensity. We noticed that the addition of 0.1 wt-% MWCNTs into the matrix highly increased the viscosity of the resin. Table 1 shows the physical properties for each fabrication condition and the measured electrical performance. For all conditions, the composite volume “ber fraction was between 38 and 43 vol-%. The hand layup process is usually not appropriate to obtain very high “ber fractions (> 60 vol.-%). This process was chosen in order to avoid alignment of the MWCNT parallel to the “bers during the impregnation process[9] and for its similarities with the prepreg process generally used in the aerospace industry.

In situ measurements of the current ”owing through each sample were also performed on the multiscale composite samples, while the electric “eld was applied. Figure 6 shows representative measurements for each loading during the application of a 60 V mm$^{-1}$ electric “eld. In both cases, the measured current increased until it reached a maximum of 150 mA after 30 min and 360 mA after 10 min for samples processed with 0.01 and 0.1 wt-% MWCNT loadings respectively. After that, the current peak values decreased and reached a plateau until the end of the experiment. The time to reach the maximum current was probably representative of the rapidity at which the MWCNT alignment occurred. The evolution of the resistivity was quite similar to that of the UV epoxy based nanocomposite samples described in the previous section, which suggests that the alignment of the MWCNTs with electric “eld is responsible for the resistivity change observed. However, it is important to emphasize that those in situ resistivity measurements do not provide an accurate measurement of the resistivity of the panel because of the presence of the release fabric between the laminate and the electrodes.

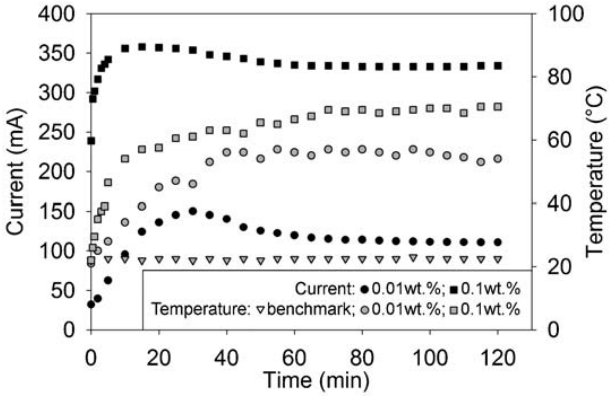


Figure 6 In situ measurements of electrical current and surface temperature of baggi ng during alignment process of multiscale composite samples

During the alignment process, the temperature of the sample was also monitored in order to evaluate the heat generation by Joule effect in the sample. Even if the electrodes and the carbon “bers were not directly in contact, a relatively high transport current (up to 360 mA) ”owed through the sample when an electric “eld of 60 V mm$^{-1}$ was applied. Figure 6 shows that the samples temperatures increased up to 55 and 70°C for MWCNT loadings of 0.01 and 0.1 wt-% respectively. A high temperature is known to reduce the viscosity of the resin, which would in principle facilitate the movement of the nanotubes, but it also reduces the gel time. At this stage of the research, it is not possible to say if this temperature increase was bene“cial or not for the nanotubes alignment.

Before performing the electrical characterization of the cured multiscale composite panels, the latter were cut in two samples of 66 × 106 × 1.25 mm, as shown in Figure 7a. In Fig. 7b, we show an optical microscopic image of the cross-section of a representative sample, in which a good “ber wetting is observed.

Electrical measurements were performed along the longitudinal and TT directions for each sample. The average resistivity for each fabrication condition is shown in Figure 7c and d. In Fig. 7c and d, we also plotted the case of a benchmark sample processed without any MWCNTs nor electric “eld and fabricated with the same set-up as the other samples. The electrical measurements and the improvements relative to the benchmark sample are also summarized in Table 1.

Table 1 Electrical properties of multiscale composite samples for each MWCNT loading and electric “eld intensity used in experiments

| MWCNT loading/ wt-% | Electric field intensity/ V mm$^{-1}$ | Average fiber fraction/ vol.-% | Longitudinal resistivity/ Ωm | Longitudinal improvement/ % | TT resistivity/ Ωm | TT improvement/ % | Resistive anisotropy ratio |
|---|---|---|---|---|---|---|---|
| 0 | 0 | 43 | 3.266 × 10$^{4}$ | N/A | 0.645 | N/A | 1980 |
| 0.01 | 0 | 40 | 4.326 × 10$^{4}$ | 2 25 | 0.634 | 2 | 1470 |
| 0.01 | 60 | 41 | 3.716 × 10$^{4}$ | 2 12 | 0.476 | 36 | 1280 |
| 0.1 | 0 | 38 | 4.276 × 10$^{4}$ | 2 24 | 0.776 | 2 17 | 1817 |
| 0.1 | 60 | 42 | 2.436 × 10$^{4}$ | 34 | 0.323 | 99 | 1330 |

Figure 7 a representative image of multiscale composite sample used for electrical characterization; b optical microscope image of cross-section of composite sample; c longitudinal and d TT resistivity of CFRPs with MWCNT loadings of 0.01 and 0.1 wt-%, processed with and without electric "eld of 60 V mm$^{-1}$ (applied for 2 h (0.01 wt-%) when used)

In the longitudinal direction, the addition of 0.01 and 0.1 wt-% of MWCNTs into the matrix without any electric "eld showed no signi"cant reduction of the resistivity in comparison to the benchmark. Nevertheless, comparisons with multiscale composites containing the same loading of MWCNTs and processed with and without an electric "eld showed a reduction of the average resistivity in the longitudinal direction by 16% and by 75% for 0.01 and 0.1 wt-% loadings respectively. The 0.1 wt-% panels fabricated with an electric "eld were the only ones showing a reduction of the longitudinal resistivity in comparison with the CFRP benchmark (34% of improvement). This slight improvement likely comes from a better current diffusion through the thickness of the material, which results in an increased effective area for electrical conduction.

In the TT direction, the addition of MWCNTs at 0.01 and at 0.1 wt-% without electric "eld did not reduce the resistivity in comparison with the CFRP benchmark. For samples containing 0.01 wt-% MWCNT loading, the TT resistivity decreased from 0.634 to 0.476 V m without and with electric "eld respectively. This correspond to an improvement of 33% compared with the 0.01 wt-% sample without electric "eld, and an improvement of 36% compared to the benchmark (0.645 V m). When the MWCNT loading was increased to 0.1 wt-%, the average TT resistivity dropped by 140%, passing from 0.776 V m (without electric "eld) to 0.323 V m (with electric "eld). This latter value corresponds to an improvement of 99% of the average TT resistivity with respect to the benchmark samples.

Globally, as the "nal result of this experiment, we did achieve an improvement by a factor of nearly two over the benchmark for the TT resistivity of the 0.1 wt-% MWCNT multiscale composites processed with an electric "eld of 60 V mm$^{-1}$. This improvement is far from our initial goal, which consisted in achieving a nearly isotropic behavior of the multiscale composite. Using numerical simulations similar as those shown in Fig. 1 for evaluating the impact of this improvement, we obtain that our best multiscale composite sample showed a reduction in the maximum power density by going from 4.3 W mm$^{-3}$ (benchmark) to 2.0 W mm$^{-3}$ (best sample). This is a good start, but it is not yet suf"cient. Obtaining a fully electrically isotropic composite panel seems to be hard to achieve and limited by the high contact resistances within the MWCNT network and between the MWCNTs and the carbon "bers.[29] However, isotropy is not necessarily needed. Our numerical simulations show that an anisotropy ratio in the range of 20…50 would be already pretty good, and that seems to be a more reasonable target for the near future and a reasonable degree of optimization of the fabrication process.

## Conclusion

In this paper, we investigated the effectiveness of using an electric "eld for aligning MWCNTs in a polymer matrix in order to fabricate: (i) nanocomposites and (ii) multiscale composites (made of carbon "ber fabrics) with reduced anisotropic behavior as compared to their present behavior (anisotropy ratio in the range of 2000). This anisotropy leads to signi"cant heating at the electrical current injection points, which prevents the composite panels to be used as current carrying media.

Our attempt to reduce this anisotropy in nanocomposite samples showed that it is possible to improve the resistivity by four orders of magnitude in a direction parallel to the electric “eld in samples containing 0.01 wt-% of MWCNTs, processed under an electric “eld of 40 V mm$^{-1}$ or higher. In the case of multiscale composite samples (CFRPs with a modi“ed matrix), the TT resistivity could be reduced by a factor of two by using an electric “eld of 60 V mm$^{-1}$ and an epoxy matrix with 0.1 wt-% of MWCNTs. In-situ measurement were performed during the application of the electric “eld and showed an increase of the sample temperature that might have in”uenced the polymerization of the resin (to be further explored). These results obtained on multiscale composites are still far from the ideal isotropic material initially sought, but it showed at least that the electric “eld alignment process is now well mastered. The remaining bottleneck is likely to be the contact resistances between the array of MWCNTs and between the MWCNTs and the carbon “bers, which does not vanish even if the “lamentary structure is well controlled. More investigation needs to be done in order to reduce these contact resistances. One possibility to achieve this goal would be to use silver coated MWCNTs.[39]

The impact of the electric “eld alignment on the mechanical properties of the samples has not been investigated in this contribution. However, an alignment of the MWCNTs through the thickness of the composite could be bene“cial, for instance, for the interlaminar shear strength of the composite.

## Conflicts of Interest

The authors have no con”icts of interest to declare.

## Acknowledgements

This project was realized with financial support from the NSERC (Natural Sciences and Engineering Research Council of Canada) and the FQRNT (Le Fonds Québécois de la Recherche sur la Nature et les Technologies).

## References

1. A. L. Goleanu, M. Dunand, J. M. Guichon, J. L. Schanen and J. L. Coulomb: •Towards the conception and optimisation of the current return path in a composite aircraft•, Proc. 2010 4th Annual IEEE Systems Conf., , San Diego, CA, USA, April 2010, IEEE, 466…471.
2. M. Arguin, F. Sirois and D. Therriault: •Impact of carbon nanotubes on electrical conductivity of carbon fiber multiscale composites•, Proc. 19th Int. Conf. on •Composite materials•, Montreal, Canada, July… August 2013, CSFCM, 8768…8776.
3. T.-W. Chou, L. Gao, E. T. Thostenson, Z. Zhang and J.-H. Byun: Compos. Sci. Technol., 2010,70, 1…19.
4. W. Bauhofer and J. Z. Kovacs: Compos. Sci. Technol., 2009,69, 1486…1498.
5. A. Moisala, Q. Li, I. Kinloch and A. Windle: Compos. Sci. Technol., 2006, 66, 1285…1288.
6. J. K. W. Sandler, J. E. Kirk, I. A. Kinloch, M. S. P. Shaffer and A. H. Windle: Polymer, 2003,44, 5893…5899.
7. F. H. Gojny, M. H. G. Wichmann, B. Fiedler, I. A. Kinloch, W. Bauhofer, A. H. Windle and K. Schulte: Polymer, 2006,47, 2036…2045.
8. J. Li, P. C. Ma, W. S. Chow, C. K. To, B. Z. Tang and J.-K. Kim: Adv. Funct. Mater., 2007,17, 3207…3215.
9. Q. Hui, E. S. Greenhalgh, M. S. P. Shaffer and A. Bismarck: J. Mater. Chem., 2010,20, 4751…4762.
10. S. S. Wicks, W. Wang and B. L. Wardle: •Influence of aligned carbon nanotube (CNT) loading on manufacturability of hybrid aligned CNT… fiber composites through vacuum assisted resin infusion•, Proc. SAMPE 2013 Conf. and Exhib.: •Education and green sky … materials technology for a better world•, Long Beach, CA, USA, May 2013, SAMPE, 1857…1863.
11. E. Bekyarova, E. T. Thostenson, A. Yu, H. Kim, J. Gao, J. Tang, H. T. Hahn, T.-W. Chou, M. E. Itkis and R. C. Haddon: Langmuir, 2007,23, 3970…3974.
12. L. Gao, T.-W. Chou, E. T. Thostenson, A. Godara, Z. Zhang and L. Mezzo: Carbon, 2010,48, 2649…2651.
13. N. Yamamoto, R. G. de Villoria and B. L. Wardle: Compos. Sci. Technol., 2012,72, 2005…2019.
14. E. F. Reia da Costa, A. A. Skordos, I. K. Partridge and A. Rezai: Composites Part A, 2012,43A, 593…602.
15. F. H. Gojny, M. H. G. Wichmann, B. Fiedler, W. Bauhofer and K. Schulte: Composites Part A, 2005,36A, 1525…1535.
16. Z. Fan, M. H. Santare and S. G. Advani: Composites Part A, 2008,39A, 540…554.
17. M. Kim, Y.-B. Park, O. I. Okoli and C. Zhang: Compos. Sci. Technol., 2009,69, 335…342.
18. D. Lefevre, S. Comas-Cardona, C. Binetruy and P. Krawczak: Compos. Sci. Technol., 2009,69, 2127…2134.
19. S. U. Khan, J. R. Pothnis and J.-K. Kim: Composites Part A, 2013,49A, 26…34.
20. A. I. Oliva-Aviles, F. Aviles, V. Sosa, A. I. Oliva and F. Gamboa: Nanotechnology, 2012,23, 465710.
21. M. Monti, M. Natali, L. Torre and J. M. Kenny: Carbon, 2012,50, 2453…2464.
22. C. Park, J. Wilkinson, S. Banda, Z. Ounaies, K. E. Wise, G. Sauti, P. T. Lillehei and J. S. Harrison: J. Polym. Sci. Part B, 2006,44B, 1751…1762.
23. Y.-F. Zhu, C. Ma, W. Zhang, R.-P. Zhang, N. Koratkar and J. Liang: J. Appl. Phys., 2009,105, 054319.
24. C. Ma, W. Zhang, Y. Zhu, L. Ji, R. Zhang, N. Koratkar and J. Liang: Carbon, 2008,46, 706…710.
25. C. A. Martin, J. K. W. Sandler, A. H. Windle, M. K. Schwarz, W. Bauhofer, K. Schulte and M. S. P. Shaffer: Polymer, 2005,46, 877…886.
26. D. Domingues, E. Logakis and A. A. Skordos: Carbon, 50, 2493…2503.
27. M. H. G. Wichmann, J. Sumfleth, F. H. Gojny, M. Quaresimin, B. Fiedler and K. Schulte: Eng. Fract. Mech., 2006,73, 2346…2359.
28. S. B. Walker and J. A. Lewis: J. Am. Chem. Soc., 2012,134, 1419…1421.
29. Y. Woo, G. S. Duesberg and S. Roth: Nanotechnology, 2007,18, 095203.
30. P. C. Ma, B. Z. Tang and J.-K. Kim: Carbon, 2008,46, 1497…1505.